PAPER • **OPEN ACCESS**

Fracture properties of concrete specimens made from alkali activated binders

To cite this article: Hana Šimonová *et al* 2017 *IOP Conf. Ser.: Mater. Sci. Eng.* **236** 012068

View the article online for updates and enhancements.

Related content

- Fracture response of alkali-activated slag mortars reinforced by carbon fibres
H Šimonová, L Topolá, P Schmid et al.
- Durability of Alkali Activated Blast Furnace Slag
K Ellis, N Alharbi, P S Matheu et al.
- Ultrasonic Monitoring Techniques of Crack Growth and Fracture Mechanics Evaluation of Materials
Hajime Nakazawa and Kazumi Hirano

IOP ebooks™

Bringing you innovative digital publishing with leading voices to create your essential collection of books in STEM research.

Start exploring the collection - download the first chapter of every title for free.

This content was downloaded from IP address 147.229.6.155 on 07/12/2018 at 09:20

IOP Conf. Series: Materials Science and Engineering **236** (2017) 012068 doi:10.1088/1757-899X/236/1/012068

Fracture properties of concrete specimens made from alkali activated binders

Hana Šimonová[1], Barbara Kucharczyková[1], Libor Topolář[1], Vlastimil Bílek, Jr.[2] and Zbyněk Keršner[1]

[1]Brno University of Technology, Faculty of Civil Engineering, Veveří 331/95, 602 00 Brno, Czech Republic
[2]Brno University of Technology, Faculty of Chemistry, Purkyňova 464/118, 602 00 Brno, Czech Republic

E-mail: kersner.z@fce.vutbr.cz

Abstract. The aim of this paper is to quantify crack initiation and other fracture properties – effective fracture toughness and specific fracture energy – of two types of concrete with an alkali activated binder. The beam specimens with a stress concentrator were tested in a three-point bending test after 28, 90, and 365 days of maturing. Records of fracture tests in the form of load versus deflection (*P–d*) diagrams were evaluated using effective crack model and work-of-fracture method and load versus mouth crack opening displacement (*P–CMOD*) diagrams were evaluated using the Double-*K* fracture model. The initiation of cracks during the fracture tests for all ages was also monitored by the acoustic emission method. The higher value of monitored mechanical fracture parameters of concrete with alkali activated blast furnace slag were achieved with substitution blast furnace slag by low calcium fly ash in comparison with substitution by cement kiln dust.

1. Introduction

Currently, the binders based on ordinary Portland cement are the most commonly used in manufacturing of concrete. At the same time, the immense emphasis is put on environment protection through reductions of CO_2 of which large quantities are produced by cement industries. Therefore, the effort to reduce CO_2 emissions is leading to develop some alternative binders among them belongs also alkali activated binders during the recent decades. These binders are formed by mixing of some aluminosilicate based material, such as blast furnace slag (BFS) or fly ash (FA), with an alkaline activator and water [1, 2]. The specific disadvantages of BFS and FA with regard to alkaline activation may be partially overcome by their mixing [3–5]. Therefore, this paper focuses on the determination of fracture parameters of concrete based on alkali activated binder which blends BFS and FA. Also a concrete based on alkali activated BFS blended with by-pass cement kiln dust (CKD) was tested.

This paper is focused on the determination of fracture parameters of above mentioned types of alkali activated binders based concrete and on their evolution in time. The records of three-point bending fracture tests of specimen with initial stress concentrator were evaluated using effective crack model, work-of-fracture method and the Double-K fracture model. The initiation of cracks during the fracture tests was also monitored by the acoustic emission method.

Content from this work may be used under the terms of the Creative Commons Attribution 3.0 licence. Any further distribution of this work must maintain attribution to the author(s) and the title of the work, journal citation and DOI.
Published under licence by IOP Publishing Ltd

2. Experimental details

Two different concrete mixtures with alkali activated binder were prepared. The both of them contained BFS, which was substituted by low calcium FA (50 %) in the first case and by CKD (25 %) in the second case. Details, regarding to material composition, specimens preparation and their curing can be found, for example, in [6].

The six specimens of the nominal dimension 75 × 75 × 295 mm were prepared from each mixture and tested in three-point bending at the age of 28 days. The three slab specimens (75 × 295 × 600 mm) were also prepared from each mixture and tested by vacuum test method. Two specimens of the nominal dimensions of 75 × 75 × 295 mm were cut from each slab (from undamaged end part of slab after vacuum tests were performed). One half of these specimens was tested in three-point bending at the age of 90 days and the second half at the age of 1 year.

The fracture experiments were conducted on beams specimens with initial stress concentrator made by a diamond blade saw before testing. The depth of initial edge notch on the bottom side of specimen was approximately 1/3 of specimen depth. The span length was 245 mm. If displacement increment loading of specimen is performed, it is possible to record the load versus displacement (*F–d*) and the load versus crack mouth opening displacement (*F–CMOD*) diagram during testing. For illustration, the *F–d* diagrams for both types of concrete made from alkali activated binder at the age of 90 days, with well recorded descending part, are shown in Figure 1.

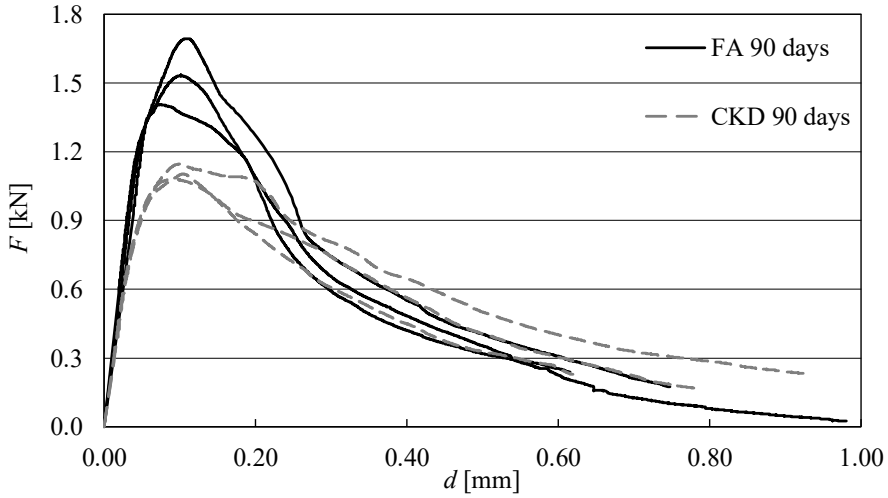

Figure 1. *F–d* diagrams of specimens tested at three-point bending at the age of 90 days.

The initiation of cracks during the fracture tests for all ages was also monitored by the acoustic emission (AE) method. The AE activity was recorded during the fracture tests. The four AE sensors were attached to the surface by beeswax. The AE signals were recorded by measuring equipment DAKEL XEDO with four acoustic emission sensors IDK-09 with 35 dB preamplifier.

The compressive strength informative values were also determined on the fragments remaining after the fracture experiments had been performed.

3. Methods

3.1. Effective crack model and work-of-fracture method

At first, almost linear part of *F–d* diagram is used to estimate modulus of elasticity value. Afterwards, the set of parameters is determined using effective crack model: critical effective crack length, effective fracture toughness and (using the known modulus of elasticity value) effective toughness [7].

The specific fracture energy value is determined from whole *F–d* diagram using the work of fracture value [8].

3.2. Double-K fracture model

The Double-*K* model [9] contains two material parameters; the first is called the initiation stress intensity factor K_{Ic}^{ini}, which defines the onset of cracking, and the second the unstable fracture toughness K_{Ic}^{un}, which defines the onset of unstable cracking or failure. These parameters characterize the tested materials in more detail and proceed from the combination of linear fracture mechanics principles and the concept of cohesive forces acting on the faces of the fictitious (effective) crack increment. In addition to the specimen dimensions and notch depth, other input data for the Double-*K* fracture model was taken from the above mentioned *F–CMOD*, namely maximum load F_{max} and its corresponding critical crack mouth opening displacement $CMOD_c$, and load F_i read from the linear part of diagram and its corresponding crack mouth opening displacement $CMOD_i$. The *F–CMOD* diagrams (part until peak load) of both tested materials at the age of 1 year are shown in Figure 2.

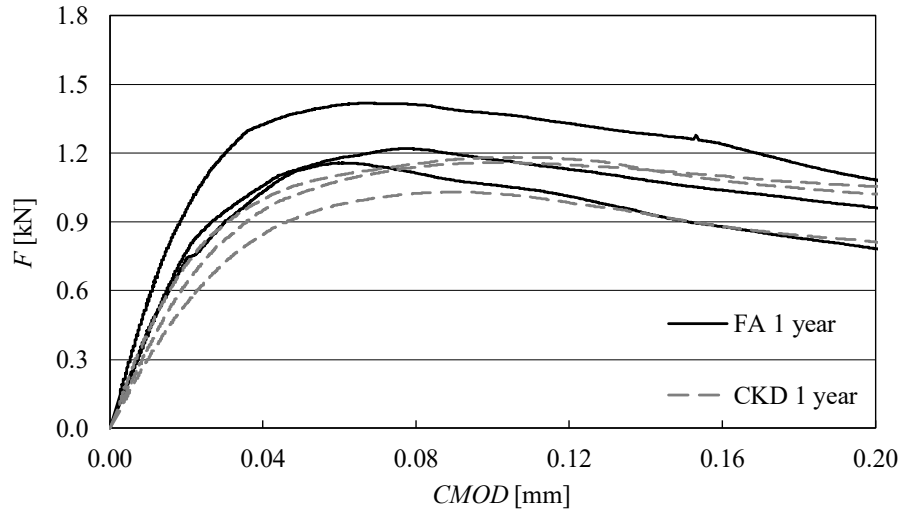

Figure 2. Part until peak load of *F–CMOD* diagrams of specimens tested at three-point bending at the age of 1 year.

In this case, the unstable fracture toughness K_{Ic}^{un} was numerically determined first, followed by the cohesive fracture toughness K_{Ic}^{c}. When both of these values were known, the following formula was used to calculate the initiation fracture toughness K_{Ic}^{ini}:

$$K_{Ic}^{ini} = K_{Ic}^{un} - K_{Ic}^{c}. \quad (1)$$

Details regarding the calculation of both the unstable and the cohesive fracture toughness values can be found in, e.g. [9, 10]. The bilinear variant [11] of the softening function was used in calculations where the tensile strength value was estimated based on the measured compressive strength value suggested by the relevant documentation [12] and the critical crack opening displacement was determined based on the fracture energy value obtained from above mentioned *F–d* diagrams.

3.3. Acoustic emission method

To describe acoustic emission signals formed during the three-point bending test, the attention is focused on the number, duration, amplitude and energy of AE signals [13]. The number of AE events corresponds to the material ability to resist fracture. The occurrence of a large number of cracks generates a rather large number of events prior to fracture. The duration of an AE signal is the time

difference between the crossing of the first and last threshold. The amplitude is the highest measured voltage in a waveform. This is an important parameter in AE inspection because it determines the detectability of the signal. Signals with amplitudes below the operator-defined limit are not recorded. Energy of AE signals is defined as an area under the envelope of the rectified linear voltage time signal from the transducer [14].

4. Results and discussion

The arithmetic mean and coefficient of variation of resulting mechanical fracture and acoustic emission parameters of both sets of concrete specimens at the age of 28, 90 days and 1 year are summarized in Table 1: bulk density γ, informative value of compressive strength f_c, modulus of elasticity E, effective crack elongation a_e–a_0, effective fracture toughness K_{Ice}, specific fracture energy G_F, unstable fracture toughness K_{Ic}^{un}, toughness ratio K_{Ic}^{ini}/K_{Ic}^{un}, i.e. the ratio of initiation fracture toughness to unstable fracture toughness, load ratio F_{ini}/F_{max}, i.e. the ratio between the force at the beginning of stable crack propagation from an initial stress concentrator and the maximal force corresponding to peak of *F–CMOD* diagram, and maximum crack tip opening displacement w_c. Mechanical fracture parameters are supplemented with parameters of AE signals, namely number of AE events N_{AE}, duration of AE signals D_{AE}, amplitude of AE signals A_{AE} and energy of AE signals E_{AE}.

Table 1. Mean values of selected parameters (coefficients of variation in %).

	FA			CKD		
	28 days	90 days	1 year	28 days	90 days	1 year
γ [kg/m^3]	2010 (0.9)	2010 (0.2)	2000 (0.4)	2230 (0.6)	2220 (0.3)	2200 (0.1)
f_c [MPa]	22.4 (2.6)	25.4 (9.8)	24.7 (5.1)	18.3 (6.3)	23.4 (9.4)	23.6 (8.8)
E [GPa]	9.6 (8.7)	7.6 (9.9)	9.4 (10.9)	5.3 (10.4)	6.0 (5.4)	6.6 (6.1)
a_e–a_0 [mm]	12.0 (22.5)	12.1 (12.0)	14.1 (8.7)	14.4 (23.7)	14.8 (11.0)	16.7 (6.0)
K_{Ice} [MPa·m$^{1/2}$]	0.579 (13.6)	0.610 (11.3)	0.553 (12.5)	0.404 (18.2)	0.497 (8.0)	0.558 (7.5)
G_F [J/m^2]	118.2 (22.0)	134.4 (18.2)	103.1 (22.8)	90.6 (19.4)	127.3 (16.9)	107.0 (25.4)
K_{Ic}^{un} [MPa·m$^{1/2}$]	0.529 (13.1)	0.680 (15.4)	0.531 (14.8)	0.382 (14.2)	0.521 (11.6)	0.537 (17.1)
K_{Ic}^{ini}/K_{Ic}^{un} [–]	0.411 (26.8)	0.311 (30.0)	0.201 (11.6)	0.139 (29.5)	0.097 (27.2)	0.129 (41.0)
F_{ini}/F_{max} [–]	0.582 (21.3)	0.547 (34.0)	0.330 (16.2)	0.224 (25.1)	0.184 (35.9)	0.235 (31.8)
w_c [mm]	0.223 (21.5)	0.233 (17.8)	0.183 (22.0)	0.177 (17.8)	0.233 (16.5)	0.194 (21.9)
N_{AE} [–]	91 (1.7)	170 (1.2)	188 (1.3)	30 (3.1)	87 (2.0)	218 (0.9)
D_{AE} [μs]	1365 (0.1)	1434 (0.2)	1310 (0.1)	1376 (0.4)	1386 (0.2)	1500 (0.2)
A_{AE} [mV]	2717 (0.3)	2900 (0.2)	2677 (0.3)	2466 (0.8)	2645 (0.3)	2571 (0.2)
E_{AE} [10^{-3}V·s]	62.9 (0.5)	124.8 (0.5)	132.0 (0.3)	29.2 (2.7)	69.8 (0.9)	180.0 (0.6)

As can be seen from Table 1, higher value of monitored mechanical fracture parameters of concrete with alkali activated BFS were achieved with substitution BFS by low calcium FA in comparison with substitution by CKD. The modulus of elasticity value is about 30–45 % lower in dependence on specimens age for CKD concrete in comparison with FA concrete. The lowest value was obtained for CKD concrete at the age of 28 days. Similar results were obtained for fracture toughness value determined by two different methods: this value is almost the same at age of 1 year for both type of concrete with alkali activated binder. In case of the ratio expressing the resistance to stable crack propagation the value is lower even about 70 % in case of CKD concrete and the value is also decreasing with age of specimens, it is almost 50 % decrease in case of FA concrete. The specific fracture energy value is also lower for CKD concrete, the trend is similar as in case of fracture toughness.

In case of AE parameters higher values were also achieved with substitution BFS by low calcium FA in comparison with substitution by CKD. In case of duration and amplitude of AE signals differences are until 10 %, whereas number of AE events and energy of AE signals shows significant differences. These two parameters were increased two times with age of specimen for FA concrete, in case of CKD concrete the increase is more than six times. It can be presumed that higher value of N_{AE} and E_{AE} indicates better mechanical properties of concrete thanks to a better bond of the matrix. The cracks of larger size generate a larger value of AE amplitude, from this point of view arises that the largest size of cracks were for specimens at the age of 90 days for both types of concrete.

5. Conclusions

The aim of this study was to quantify the influence of fly ash (FA) and by-pass cement kiln dust (CKD) on mechanical fracture parameters of alkali activated BFS concrete and their comparison for different age of specimens.

The mechanical fracture parameters of alkali activated binder based concrete were higher in the case of substitution BFS by FA compared to CKD. With exception of resistance to stable crack propagation, other monitored parameters were increased with age of specimens. The slight decrease of some parameters of FA concrete was monitored at the age of 1 year.

The AE technique was used to monitor the specimens failure during the experiments. It is evident, that different types of cracks generate different AE signals. In summary, the results of the experiments conducted as part of this project can be used to infer properties of materials as well as the specific characteristics of micro-cracks. The properties of the micro-cracks can ultimately be linked to the overall behavior of the building materials under stress.

Acknowledgements

This outcome has been achieved with the financial support of the Competence Centre programme of the Technology Agency of the Czech Republic (TACR) within the project Centre for Effective and Sustainable Transport Infrastructure (CESTI), project no. TE01020168, and with financial support from the Czech science foundation, project no. GA17-03670S Development of shrinkage reducing agents designed for alkali activated systems.

References

[1] Provis J L and van Deventer J S (eds) 2014 *Alkali activated materials: state-of-the-art report, RILEM TC 224-AAM* (Dordrecht: Springer)

[2] Shi C, Krivenko P V and Roy D 2006 *Alkali-activated cements and concretes* (London: Taylor & Francis)

[3] Marjanović N, Komljenović M, Baščarević Z, Nikolić V and Petrović R 2015 Physical–mechanical and microstructural properties of alkali-activated fly ash–blast furnace slag blends *Ceramics International* **41** pp 1421–35

[4] Chi M and Huang R 2013 Binding mechanism and properties of alkali-activated fly ash/slag mortars *Construction and Building Materials* **40** pp 291–98

[5] Aydin S 2013 A ternary optimisation of mineral additives of alkali activated cement *Construction and Building Materials* **43** pp 131–38

[6] Bílek V Jr, Šimonová H, Havlíková I, Topolář l, Kucharczyková B and Keršner Z 2017 Alkali Activated Binders Based Concrete Specimens: Length Change and Fracture Tests *Solid State Phenomena: Materials Structure & Micromechanics of Fracture VIII (Brno)* ed P Šandera (Switzerland: Trans Tech Publications) **258** pp 623−6

[7] Karihaloo B L 1995 *Fracture Mechanics and Structural Concrete* (New York: Longman Scientific & Technical)

[8] RILEM TC-50 FMC Recommendation 1985 Determination of the fracture energy of mortar and concrete by means of three-point bend test on notched beams *Materials & Structures* **18** pp 285–90

[9] Kumar S and Barai S V 2011 *Concrete Fracture Models and Applications* (Berlin: Springer)
[10] Reinhardt H W, Cornelissen H A W and Hordijk D A 1986 Tensile tests and fracture analysis of concrete *Journal of Structural Engineering* **112** pp 2462–77
[11] Petersson P E 1981 *Crack growth and development of fracture zone in plain concrete and similar materials Report No. TVBM-1006* (Lund Institute of Technology)
[12] Červenka V, Jendele L and Červenka J 2014 *ATENA Program documentation – Part 1: Theory* (Prague: Cervenka Consulting)
[13] Grosse C U and Ohtsu M 2008 *Acoustic Emission Testing: Basics for Research – Applications in Civil Engineering; with contributions by numerous experts* (Heidelberg: Springer)
[14] Sagar R V 2009 An experimental Study on Acoustic Emission Energy and Fracture Energy of Concrete *Proc. of the National Seminar & Exhibition on Non-Destructive Evaluation (Tiruchirappalli, India)* pp 225–8